Pham and Oh *Int. J. Air-Cond. Ref.* (2022) 30:14
https://doi.org/10.1007/s44189-022-00014-4

International Journal of
Air-Conditioning and Refrigeration

RESEARCH Open Access

Flow condensation heat transfer of propane refrigerant inside a horizontal micro-fin tube

Quang Vu Pham[1] and Jong-Taek Oh[2*]

Abstract

Due to the phase-out of CFCs and HCFC refrigerants, propane is a nature refrigerant occurring substance produced by natural gas production and oil refining. As a result, propane has a higher latent heat and lower density than conventional refrigerants while maintaining a comparable saturation pressure and thermal conductivity. So, propane refrigerant is already widely used in domestic fridges and freezers for many years. However, propane's operating pressures and temperatures are well suited for air conditioning equipment, including chillers. This study investigates the contributions of different heat transfer mechanisms in two-phase flow condensation heat transfer coefficients for propane inside a 6.3-mm ID micro-fin copper tube. Data were collected through an experiment with a two-phase flow condensation. Measurements were taken at different refrigerant mass fluxes from 100 to 300 kg/m^{2}s and heat fluxes from 3 to 9 kW/m^2. In addition, the experiments investigated effect of vapor quality, mass flux, and heat flux on the heat transfer coefficients. Finally, a new heat transfer coefficient correlation was developed based on the experimental data with good agreement.

Keywords: Propane, Condensation, Heat transfer coefficient, Correlation, Micro-fin tube

1 Introduction

In the future, hydrocarbons may be widely used as refrigerants due to their desirable thermodynamic and transport properties, resembling HFC refrigerants. Furthermore, natural refrigerants have minimal environmental effects compared to all synthetic refrigerants, but the flammability of hydrocarbons is a significant drawback. Propane refrigerant (R-290) with the chemical formula C_3H_8 is a natural and efficient refrigerant with a very low GWP and ODP=0, no damage to the ozone layer, and the minimal greenhouse effect.

On the other hand, propane has a higher latent heat and lower density than conventional refrigerants while maintaining a comparable saturation pressure and thermal conductivity. The advantage of R-290 is the lowest compression ratio when operating in low evaporating temperature mode because it limits the compressor discharge temperature that affects the lubricating oil and saves energy. Therefore, propane is regarded as a long-term alternative refrigerant. Its employment in refrigeration applications represents an interesting opportunity as the physical properties are close to R22. Furthermore, it is one of the most environmentally friendly refrigerants, used as an alternative to R404A and R407 series refrigerants in new refrigeration and air conditioning systems.

Through much research, refrigerant condensing behavior in horizontal tubes is well understood, and some correlations have been proposed. Several researchers, such as Kim [1], Islam et al. [2], and Wijaya [3], compared the heat transfer coefficients of R410A and R22 flow inside smooth and micro-fin tubes. They conclude that the heat transfer coefficient of R22 and R410A are almost similar in smooth tubes, and the heat transfer coefficients of R410A are lower than those of R22 in micro-fin tubes. Hossain, Onaka, and Miyara [4]; López-Belchí [5]; and Guo and Anand [6] also studied the condensation heat transfer of R32 and R410A inside mini and

*Correspondence: ohjt@chonnam.ac.kr

[2] Department of Refrigeration and Air-Conditioning Engineering, Chonnam National University, 50 Daehak-ro, Yeosu, Chonnam 59626, Republic of Korea
Full list of author information is available at the end of the article

conversational channel tubes. They reported that the heat transfer performance of R32 is higher than that of R410A due to the higher thermal conductivity of R32. Zhang et al. [7] tested the R410A condensation heat transfer and pressure drop inside a micro-fin and smooth tubes with an OD of 5mm. The experiment was conducted on a mass flux range of 390–1583kg/m^{2}s with saturation temperatures of 309.15K, 316.15K, and 323.15K. The authors showed that the heat transfer coefficient increases with decreasing condensing temperatures due to increased shear forces and surface tension. Wen et al. [8] investigated heat transfer and pressure drop of R600, R600/R290 (50%/50%), and R290 in the three-line serpentine small-diameter 2.46mm experimentally. They reported that the heat transfer coefficient for R600, R290/R600, and R290 is about 155%, 124%, and 89% larger than R134A at the same conditions. Del Col, Torresin, and Cavallini [9] measured the heat transfer coefficient, the pressure drop of propane during condensation, and boiling in a mini-channel tube. They found that the experimental heat transfer coefficient is well predicted using the model by Cavallini [10]. In the study of Kedzierski and Kim [11], the convection boiling and condensation of R12, R22, R152a, R134a, and R290 inside a circular 9.72 mm tube are presented. They found that the measured condensation heat transfer coefficient decreases for most of the data for decreasing vapor qualities.

The present study aims to provide a comprehensive experimental characterization of the performance of propane during the condensing process in a micro-fin copper tube with a 6.3-mm inner diameter at the saturation temperature of 48°C for mass fluxes of 100 to 300kg/m^{2}s and heat fluxes of 3–9kW/m^2. Given this background from the literature, the present study aims to provide a comprehensive experimental characterization of the heat transfer performance of propane during condensation in a micro-fin tube.

2 Experimental apparatus and data reduction

Figure 1 is a schematic of the experimental setup of the present study. The experimental facility consists of refrigerant and cooling water loops. The refrigerant loop consists of four major sections: the sub-cooled, the pre-heater, the test section, and the post-condensers. The sub-cooled is included a sub-cooler, a refrigerant gear pump, and a Coriolis-type mass flow meter. The sub-cooler is a tube-in-tube heat exchanger with refrigerant flow inside the tube and a cooling water loop; a water-cooling loop cools the refrigerant to achieve a subcooled state. The subcooled temperature of refrigerants is controlled by setting the temperatures of constant temperature baths connected with the sub-cooler. The refrigerant is circulated in the refrigerant loop by a

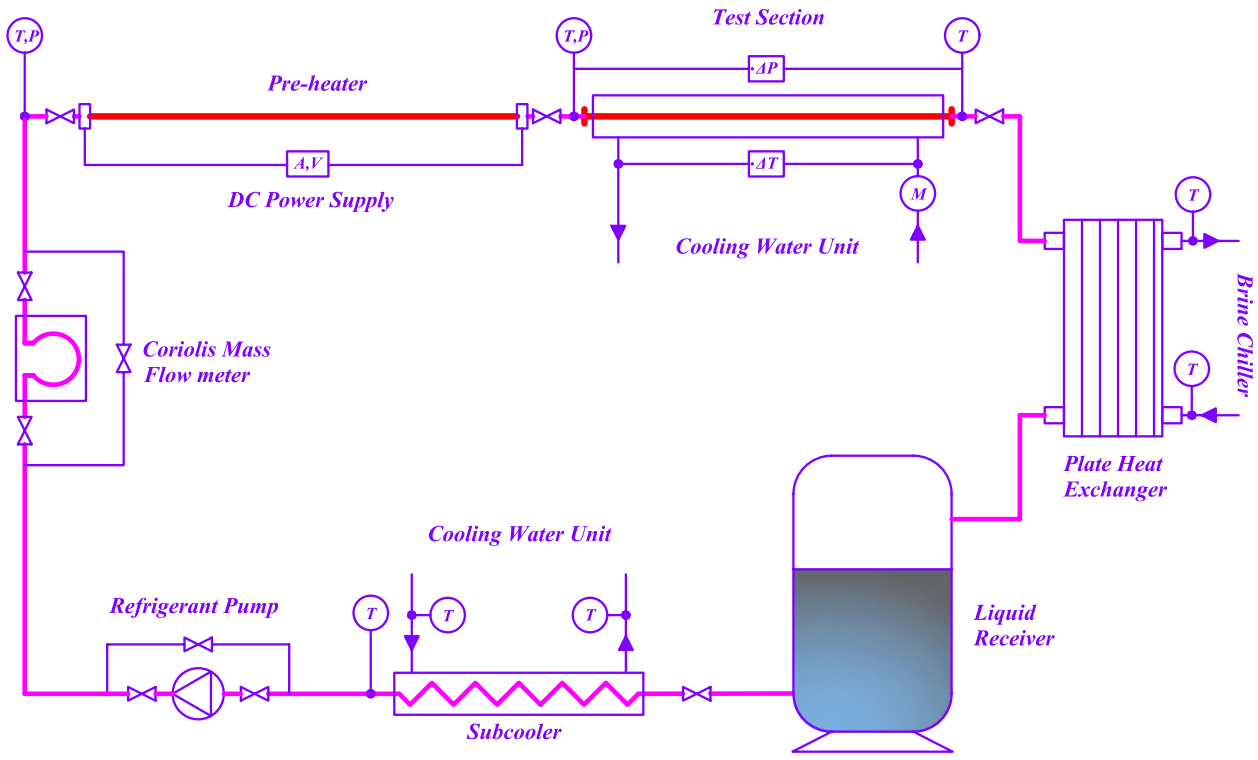

Fig. 1 Experiment apparatus

magnetic micro-gear pump. The saturation temperature of refrigerant was maintained at 48°C at the inlet of the test section and measured using a pressure gauge and a platinum resistance thermometer. The pre-heater was set up to control the saturation temperature and vapor quality using a DC power supply. The aims of the subcooled part provided the subcooled state refrigerant and required mass flow rate.

Figure 2 shows the details of the test section. The test section was designed as a horizontal counterflow tube in the tube heat exchanger with a total length of 1.7m. The test section tube consisted of 2 sub-sections: a 0.5-m isothermal section and a 1.2-m condensation section. The insulated isothermal test section stabilized the refrigerant flow pattern inside the test tube. In the test section, a counterflow tube-in-tube condenser, the refrigerants flow inside the micro-fin tube while the cooling water flows on the annulus side. The outer tube is a PVC tube with a 17-mm inner diameter. The heat transfer rate between the cooling water and refrigerant flow condensing inside test tubes is varied by adjusting the inlet cooling water temperature. The mass flow rate of cooling water is kept constant at 1kg/min. Three absolute pressure transmitters and two differential pressure transducers were connected to three pressure taps located along the test section to evaluate the static pressure and pressure drop, respectively. The tube wall temperatures were measured using twelve T-type thermocouples that were welded at three points in the cross-section of the test section (top, middle, and bottom). All the T-type thermocouples in the experimental model were calibrated before installation; the estimated uncertainty of the thermocouple measurement is ±0.1K.

Figure 3 demonstrates the attachment of T-Type thermocouples on the micro-fin surface where the outer tube wall temperatures were measured. The water temperature was measured by two platinum resistance thermometers installed at the inlet and exit of the water annulus. The uncertainty of the platinum resistance thermometer measurements was estimated to be within 0.01K. The heat balance between the inside fluids and the cooling water on the annulus side is checked carefully with both fluids using water. The heat balance in the test section and pre-heater was described in Figs. 4 and 5, with a difference of less than 3%. Also, two sight glasses were set up on two sides of the test sections to watch the flow patterns of refrigerants with the same inner diameters as the micro-fin tubes. A high-speed camera was also set up at the exit of the test section.

The local heat fluxes are determined by the temperature sensors attached along the length of test sections. The initial experiment with the liquid water-water test showed that the variation of local heat fluxes along the test section length is negligible. So, it can be assumed that the heat flux on the test section is uniform. The average heat flux in the test section was determined as follows:

$$q = \frac{m_{water} C_{p,water} \Delta T_{water}}{A_{internal}} \tag{1}$$

where m_{water} is the cooling water mass flow rate, ΔT_{water} is the temperature difference between the inlet and outlet of the cooling water side, and $A_{internal}$ is the internal surface area of the test section tube. The cooling water mass flow rate in all cases is fixed at 1 kg/min to maintain the water flow distribution on the annulus side. The inlet cooling water controls the heat flux value, controlled by the chiller unit connected to the test section. Depending on the specific cases, the inlet cooling water temperature is adjusted from 42.56 to 45.18°C.

The equation calculated the heat transfer coefficient:

$$h = \frac{Q}{A\left(T_{sat} - T_{w,i}\right)} \tag{2}$$

The vapor quality of refrigerant at the inlet of the test section was controlled by controlling the power of the DC power supply. The vapor quality difference in the test section is approximate 0.011 to 0.16. Therefore, it can be assumed that the variation in vapor quality in the test section is linear over the length of the test section. The below equation calculates the vapor quality in the test section:

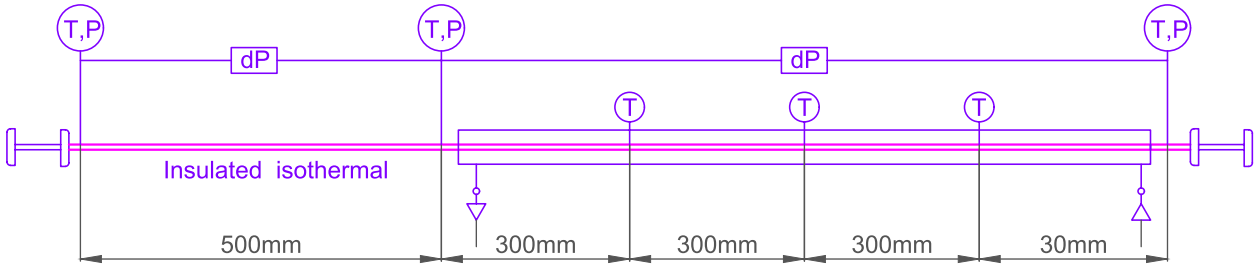

Fig. 2 Detail of the test section

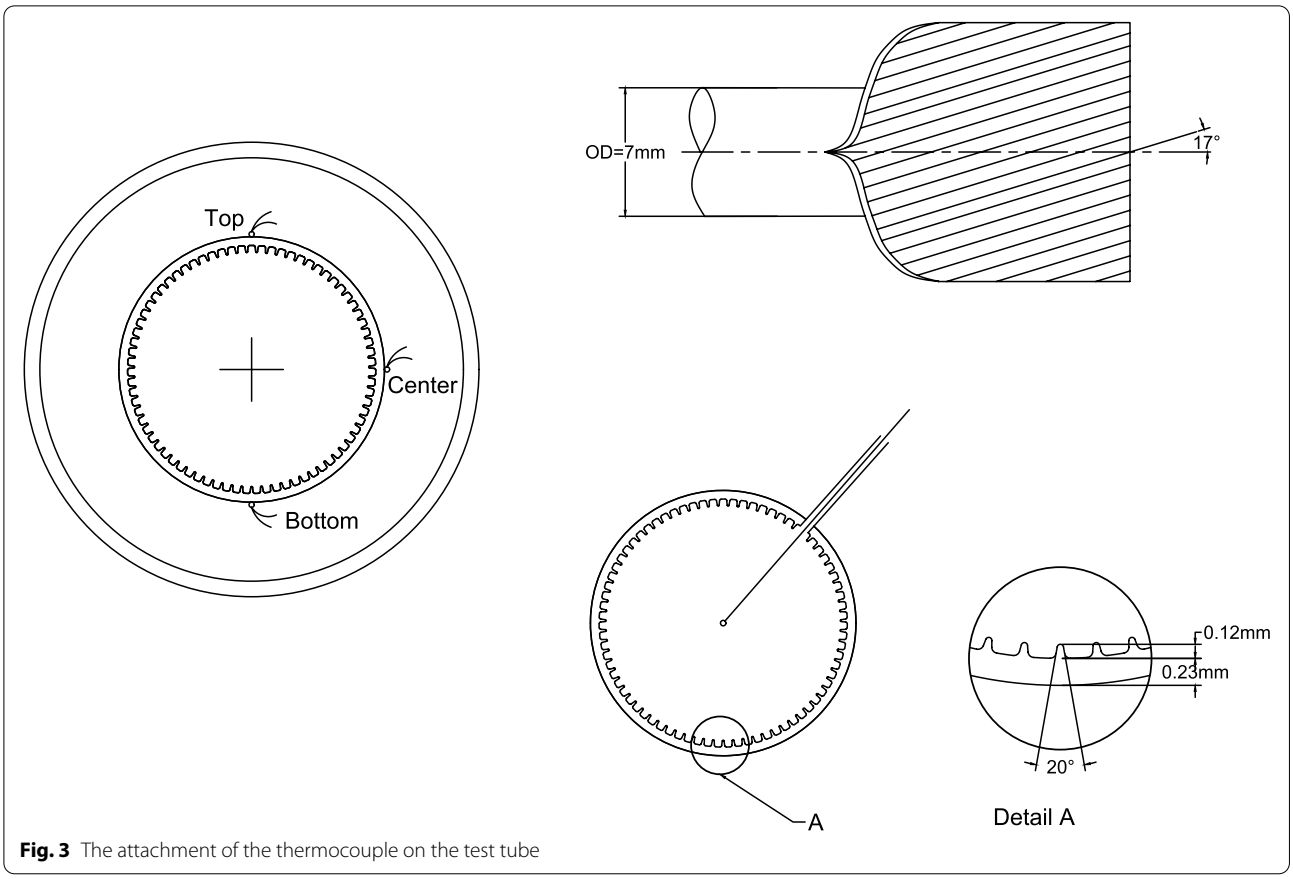

Fig. 3 The attachment of the thermocouple on the test tube

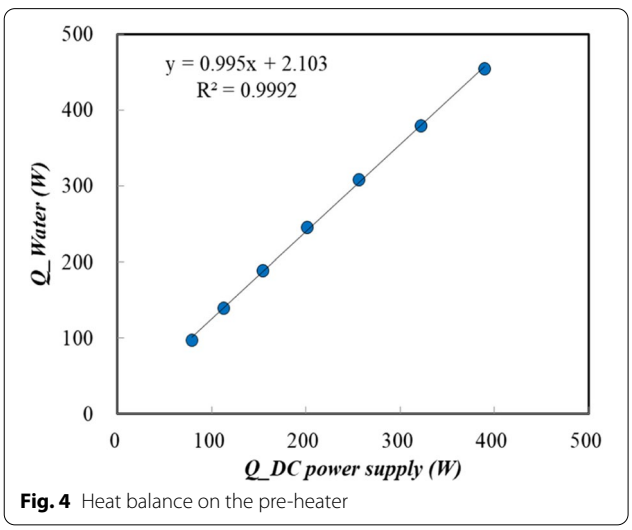

Fig. 4 Heat balance on the pre-heater

$$x_{in} = \frac{1}{h_{fg}}\left(\frac{Q_p}{m_r} - C_{pr}\left(T_{sat} - T_{p,in}\right)\right) \tag{3}$$

The inner wall temperature determined to follow the Fourier steady-state one-dimensional heat conduction through the tube wall was calculated as equations:

$$T_{w,i} = T_{w,o} + \frac{q}{2\pi k_{copper}}\ln\left(\frac{d_o}{d_i}\right) \tag{4}$$

where k is the thermal conductivity of the tube's material, and through all the date reduction processing, the different temperatures between the inside and outside wall tubes were less than 0.025K.

All the temperature sensors were calibrated against it with an accuracy of ±0.01K with RTDs and ±0.1K with thermocouples. The refrigerant saturation temperatures were determined by measuring saturation pressures at the inlet of the condenser tubes. Three absolute pressure transducers were installed at the pre-heater's inlet and the outlet of the test section. They measured the static pressure with ±2.5kPa for uncertainty, combined with a differential pressure transducer with an accuracy of ±0.25% (0.1kPa). During the condensation experiment, the heat balance between the inside fluid and outside water was carried out, and the heat loss was less than 4%. The uncertainties of heat transfer coefficients were related to accurately measuring temperature, pressure, mass flux, and heat flux.

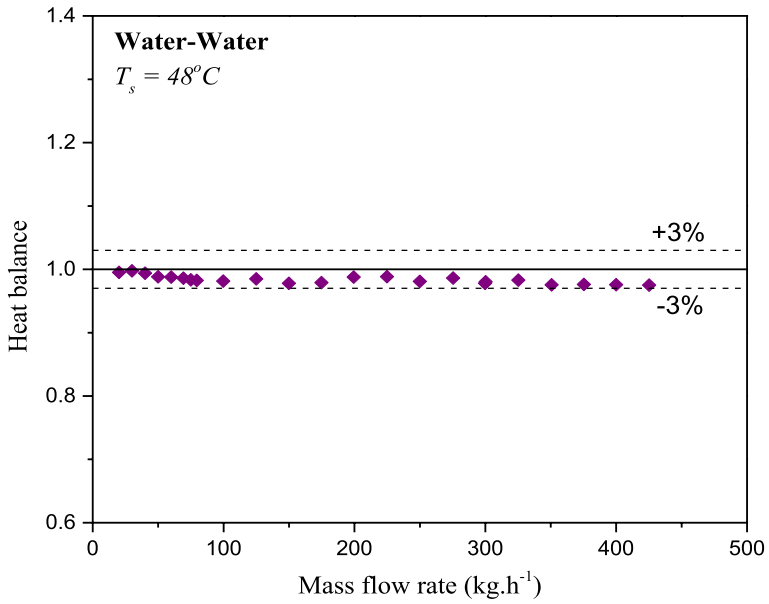

Fig. 5 Heat balance on the test section

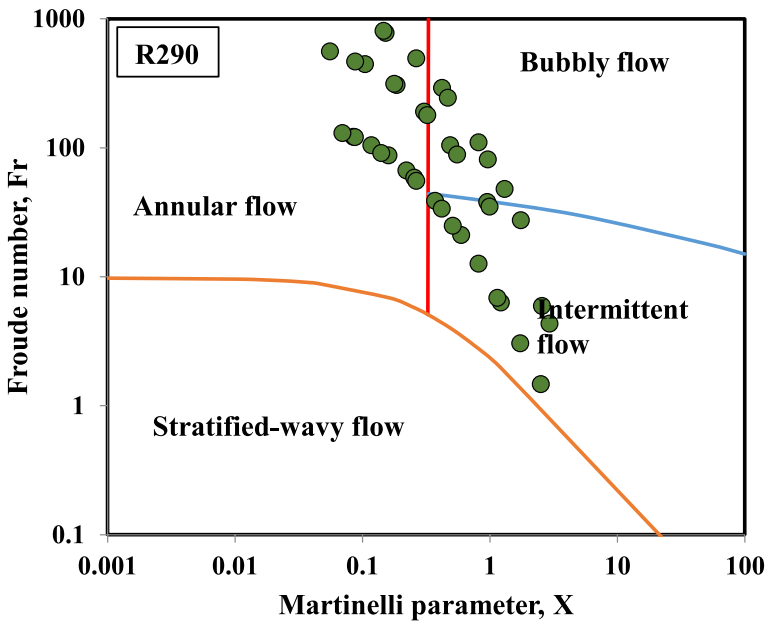

Fig. 6 Experimental data of R290 overlaid on the Taitel-Dukler (1976) flow pattern map

The physical properties of the refrigerants in data reduction of the present study were calculated using the REPROP version 8.0.

3 Results and discussion

Figures 6 and 7 present the observed flow patterns on the Taitel and Dukler's [12] and El Hajal, Thome, and

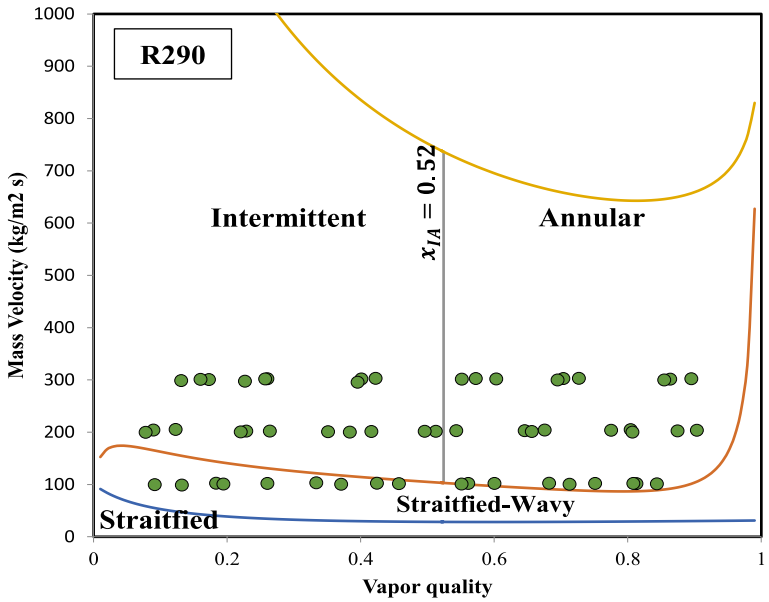

Fig. 7 Experimental data of R290 overlaid on the Hajal et al. (2003) flow pattern map

Cavallini's [13] flow pattern map. The prediction of the Taitel and Dukler [12] map shows all of the experimental points located in annular and intermittent flow, as shown in Fig. 6. Figure 7 shows that a mass flux of 100kg/m^{2}s, the data points lay in the stratified-wavy regime with vapor quality lower than 0.52 and lay in the annular regime with vapor quality higher than 0.52. The quick change of flow regime at a low mass flux of propane can be explained by the small density ratio of the vapor and liquid phases, resulting in a significant velocity difference between the liquid and vapor phases. When mass flux is higher than 100kg/m^{2}s, the flow pattern is in the intermitted and annular flow with the flow transition as a vertical line $x_{IA}=0.52$. El Hajal, Thome, and Cavallini [13] concluded that the transitional vapor quality (x_{IA}) between intermittent and annular flows is a density and viscosity ratio function. If the density and viscosity ratio is high, the value x_{IA} will be higher. The visualization of the two-phase flow in the test section is recorded using a high-speed camera installed in the sight glass at the outlet of the test section tubes. During high-speed camera recording, all the test conditions are maintained at a fixed value, such as the mass flow rate, heat flux, and vapor quality. The liquid phase flow patterns observed at the vapor quality of about 0.6, at the mass flux is 100kg/m^{2}s are mainly located at the bottom of the tube. Also, the waves occurred at the interface between the liquid and vapor phases. Its phenomena are the stratified wavy flows. The intermittent flow occurred at a higher mass flux regime when the waves between the liquid and vapor phases developed too big enough to reach the top of the tube. At mass fluxes higher than 100kg/m^{2}s and

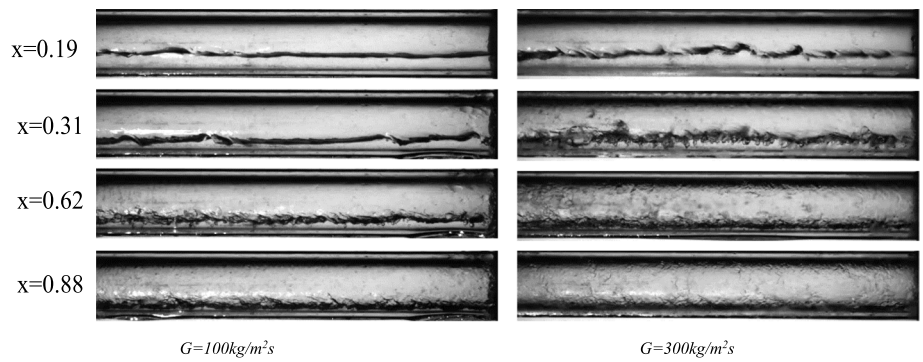

Fig. 8. Two-phase flow patterns on the variable of mass flux and vapor quality of R290 in micro-fin tube

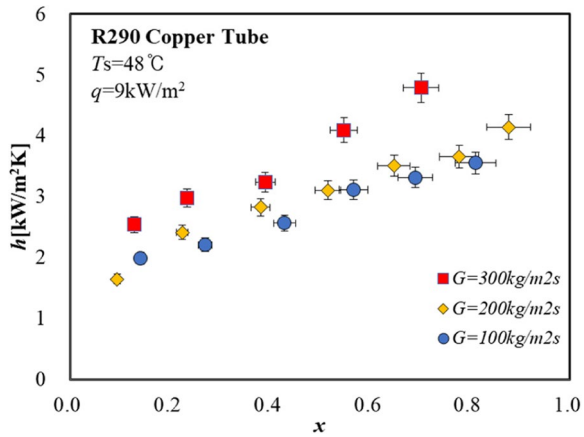

Fig. 9 The effect of mass flux on the heat transfer coefficients

high vapor quality, the liquid film occurred around the perimeter of the tubes, and the vapor flows in the center of the tube, which means the flow pattern is annular flow. Figure 8 demonstrated the flow pattern of R290 during condensation with the variable of mass flux and vapor quality.

This phenomenon is a small difference compared to the experimental data and the flow pattern map proposed by El Hajal, Thome, and Cavallini [13], which was developed for conventional plain tubes. However, it means that the flow pattern development inside the micro-fin tube is slower than that of the plain tube.

Figure 9 shows the heat transfer coefficient influence of mass flux inside a 6.3-mm ID micro-fin tube. The increase in vapor quality and mass flux leads to the condensation heat transfer coefficient increase because of the forced convection mechanism. The forced convection contribution is dominant with high vapor qualities and mass fluxes. Moreover, the flow pattern located in the annular flow regime, as the vapor quality increases, the thickness of the liquid film becomes thinner, which reduces thermal resistance and increases heat transfer coefficients. Jung et al. [14] and Byun et al. [15] reported the same phenomena. They explained that it is due to a decreased thermal conduction resistance in the liquid film with the rising mass flux and vapor quality. In the case of low mass flux, the entrance region flow is annular, but this quickly transforms into the intermittent or stratified flow. The regimes are characterized by large-amplitude waves rising on the top side of the horizontal tube or changing to stratified-wavy flow with smaller amplitude waves.

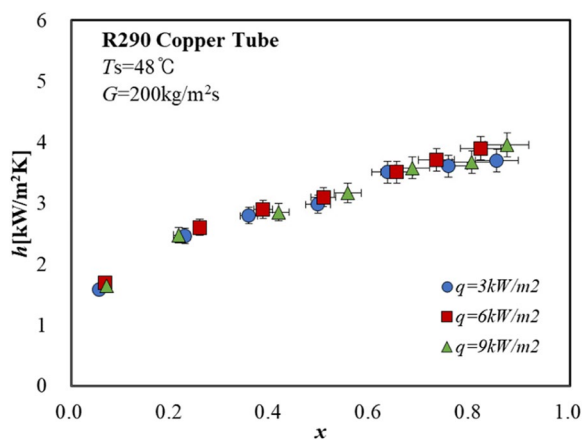

Fig. 10 The effect of heat flux on the heat transfer coefficients

The effect of heat flux on the condensation heat transfer coefficient is presented in Fig. 10. It is seen that the heat flux is having an insignificant impact on the variable of heat flux.

Table 1 compares experimental condensation heat transfers with the existing correlations. The Bivens and Yokozeki [16] and Kedzierski and Goncalves [17] correlations give acceptable predictions with measurement data. Bivens and Yokozeki [16] and Kedzierski and Goncalves [17] proposed heat transfer coefficient correlations in the case of forced convection condensation, which were developed for annular flow patterns. It under-predicted the experimental data, with almost all data lying in the annular regime. However, in other flows, the regime shows over-prediction. Bivens and Yokozeki's [16] correlation shows the best fit with an absolute mean deviation of 13.8%. This correlation was generated using R22, R32/R134a, R32/R125/R134a, and R502 condensation inside a horizontal 8-mm OD tube and correlated their results to Shah's [18] correlation with the modified empirical term.

However, a new coefficient correlation was developed based on the experimental data to improve the predicted heat transfer coefficient. The new correlation was defined as follows:

Table 1 Heat transfer coefficient comparison

Correlations	MD (%)	AD (%)
Akers (1959)	33.45	−27.41
Dobson (1994)	33.92	25.36
Shah (1978)	30.28	19.24
Bivens and Yokozeki (1994)	13.80	5.57
Tang (2000)	28.76	9.48
Kaushik and Azer (1988)	17.98	14.30
Kedzierski and Goncalves (1999)	14.67	−1.68
Yu and Koyama (1998)	52.27	51.10
Thome et al. (2003)	36.13	15.64

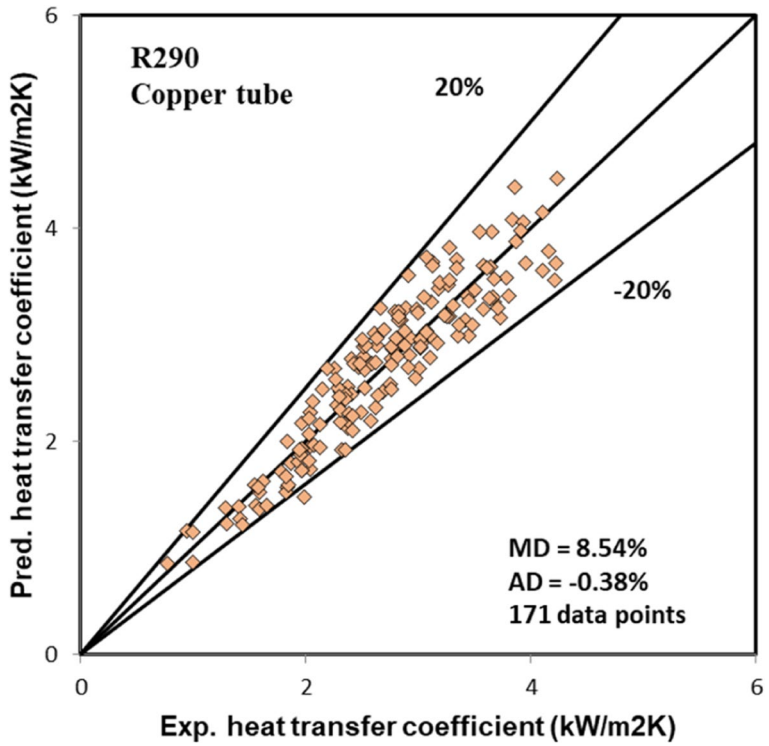

Fig. 11 Comparison between the measured data and new heat transfer coefficient correlation

$$h = \frac{k_l}{D_i} 0.007079 \mathrm{Re}^{0.1112} Ja^{-0.232x} \mathrm{Pr}^{-0.68} P_r^{-0.578x^2} \left(-\log(\mathrm{Pr})\right)^{-0.474x^2} Sv^{2.531x} \quad (5)$$

where Re is Reynolds number of all flow as a liquid

$$\mathrm{Re} = \frac{GD_i}{\mu_l} \quad (6)$$

Ja is refrigerant Jacob's number

$$Ja = \frac{h_{fg}}{C_{p,l}\Delta T_s} \quad (7)$$

Pr is the liquid refrigerant Prandtl number is calculated as follows:

$$\mathrm{Pr} = \frac{C_{p,l}\mu_l}{k_l} \quad (8)$$

P_r is the refrigerant reduced pressure as follows:

$$P_r = \frac{P_{saturation}}{P_{critical}} \quad (9)$$

S_v is the dimensionless specific volume that can be obtained as follows:

$$Sv = \frac{v_g - v_l}{v} = \frac{v_g - v_l}{xv_g + (1-x)v_l} \quad (10)$$

The comparison between the measured heat transfer coefficient with the predicted value calculated from the newly proposed correlation is presented in Fig. 11. The proposed correlation shows a good prediction with a mean deviation of 8.54%.

4 Conclusion

Flow condensation heat transfer of R290 in a micro-fin tube was investigated experimentally. The results are summarized as follows:

- The transition between the annular flow and the intermitted flow in micro-fin tubes is slower than in the plain tube.
- The effects of vapor quality, mass flux, and heat flux on the condensation heat transfer coefficient were studied. The heat transfer coefficient increases with vapor quality and mass flux, but heat flux has an insignificant impact.
- A new heat transfer coefficient correlation was developed based on the experimental data with the mean and average deviations of 8.54% and 0.38%, respectively.

Acknowledgements
This work is supported by the National Research Foundation of Korea (NRF) grant funded by the Korean government (MIST) (No. NRF-2020R1A2C1010902).

Authors' contributions
VP performed heat transfer coeficient experiments and drafted the manuscript. OJ conceived of the study and participated in its design and coordination. All authors read and approved the final manuscript.

Availability of data and materials
All data generated or analyzed during this study are included in this published article.

Declarations

Competing interests
The authors declare that they have no conflict of interest.

Author details
[1]Faculty of Energy Technology, Electric Power University, Hanoi 10000, Vietnam. [2]Department of Refrigeration and Air-Conditioning Engineering, Chonnam National University, 50 Daehak-ro, Yeosu, Chonnam 59626, Republic of Korea.

Received: 17 June 2022 Accepted: 19 October 2022
Published online: 16 November 2022

References

1. Kim, N.-H. (2016). Condensation of R-134a on horizontal enhanced tubes having three-dimensional roughness. *International Journal of Air-Conditioning and Refrigeration, 24*, 1650013.
2. Islam, M. A., & Miyara, A. (2007). Liquid film and droplet flow behaviour and heat transfer characteristics of herringbone microfin tubes. *International Journal of Refrigeration, 30*, 1408–1416.
3. Wijaya, H. (1994). Two-phase flow condensation heat transfer and pressure drop characteristics of HCFC-22 and AZ-20. In *International refrigeration and air conditioning conference at Purdue* (pp. 305–310).
4. Hossain, M. A., Onaka, Y., & Miyara, A. (2012). Experimental study on condensation heat transfer and pressure drop in horizontal smooth tube for R1234ze(E), R32 and R410A. *International Journal of Refrigeration, 35*, 927–938.
5. López-Belchí, A. (2019). Assessment of a mini-channel condenser at high ambient temperatures based on experimental measurements working with R134a, R513A and R1234yf. *Applied Thermal Engineering, 155*, 341–353.
6. Guo, Z., & Anand, N. K. (2000). An analytical model to predict condensation of R-410A in a horizontal rectangular channel. *Journal of Heat Transfer, 122*, 613.
7. Zhang, J., Zhou, N., Li, W., Luo, Y., & Li, S. (2018). An experimental study of R410A condensation heat transfer and pressure drops characteristics in microfin and smooth tubes with 5 mm OD. *International Journal of Heat and Mass Transfer, 125*, 1284–1295.
8. Wen, M.-Y., Ho, C.-Y., & Hsieh, J.-M. (2006). Condensation heat transfer and pressure drop characteristics of R-290 (propane), R-600 (butane), and a mixture of R-290/R-600 in the serpentine small-tube bank. *Applied Thermal Engineering, 26*, 2045–2053.
9. Del Col, D., Torresin, D., & Cavallini, A. (2010). Heat transfer and pressure drop during condensation of the low GWP refrigerant R1234yf. *International Journal of Refrigeration, 33*, 1307–1318.
10. Cavallini, A., et al. (2006). Condensation in horizontal smooth tubes: a new heat transfer model for heat exchanger design. *Heat Transfer Engineering, 27*, 31–38.
11. Kedzierski, M. A., & Kim, M. S. (1998). Convective boiling and condensation heat transfer with a twisted-tape insert for R12, R22, R152a, R134a, R290, R32/R134a, R32/R152a, R290/R134a, R134a/R600a. *Thermal Science and Engineering, 06, 113–122.*
12. Taitel, Y., & Dukler, A. E. (1976). A model for predicting flow regime transitions in horizontal and near horizontal gas-liquid flow. *AIChE Journal, 22*, 47–55.
13. El Hajal, J., Thome, J. R., & Cavallini, A. (2003). Condensation in horizontal tubes, part 1: two-phase flow pattern map. *International Journal of Heat and Mass Transfer, 46*, 3349–3363.
14. Jung, D., Song, K. H., Cho, Y., & Kim, S. J. (2003). Flow condensation heat transfer coefficients of pure refrigerants. *International Journal of Refrigeration, 26*, 4–11.
15. Byun, H.-W., Lee, E.-J., Sim, Y.-S., Lee, J.-K., & Kim, N.-H. (2013). Condensation heat transfer and pressure drop of R-410a in a 5.0 Mm O.D. Smooth and Microfin Tube. *International Journal of Air-Conditioning and Refrigeration, 21*, 1350018.
16. Bivens, D. B., & Yokozeki, A. (1994). Heat transfer coefficients and transport properties for alternative refrigerants. *Proceeding International Refrigeration and Air Conditioning Conference, 299–304*
17. Kedzierski, M. A., & Goncalves, J. M. (1999). Horizontal convective condensation of alternative refrigerants within a micro-fin tube. *Journal of Enhanced Heat Transfer, 6*, 161–178.
18. Shah, R. K., & London, A. L. (1972). *Flow forced convection heat transfer and flow friction in straight and curved ducts - a summary of analytical solutions* (Vol. 1, p. 311).

Publisher's Note